Volcanic aerosol layers observed with multi-wavelength Raman lidar over Europe since summer 2008

Ina Mattis, Patric Seifert, Detlef Müller, Matthias Tesche, Anja Hiebsch, Thomas Kanitz, Jörg Schmidt, and Fanny Finger

Leibniz Institute for Tropospheric Research, Permoser Str. 15, 04318 Leipzig, Germany, ina@tropos.de

ABSTRACT

In the framework of regular EARLINET observations aerosol layers can be observed in the upper troposphere - lower stratosphere (UTLS) region above Europe since summer 2008. FLEXPART transport simulations show that the origin of those layers are eruptions of different volcanoes on the Aleutian Islands, Kamchatka, Alaska, and on the Kuril Islands. The aerosol layers extended up to a maximum height of 30 km whereas the strongest aerosol layers could be found in the tropopause region. Optical depth at 532 nm was in the range between 0.004 and 0.016. Multi-wavelength Raman lidar observations over Leipzig show a strong wavelength dependence of the backscatter coefficients and extinction coefficients. Lidar ratios at 355 nm are significantly larger than those at 532 nm. The effective radius was estimated to be 0.1μm.

1. INTRODUCTION

Regular multi-wavelength Raman lidar observations of the vertical aerosol distribution have been performed at the Leibniz Institute for Tropospheric Research (IfT), Leipzig, Germany since 1996. Our measurements in the past 12 years did not show any major event of volcanic aerosol pollution in the UTLS region (1). The situation changed due to a series of strong eruptions of volcanoes on the Aleutian Islands, Kamchatka, Alaska, and on the Kuril Islands since summer 2008. Table 1 lists the corresponding volcanoes, their location, and the estimated maximum height of the emitted gas or ash plumes. All volcanoes are located between 40 °N and 70 °N. The eruption dates can be seen from Fig. 1.

It has been observed after previous major volcanic eruptions (e.g., El Chichon and Pinatubo) that the transport of volcanic aerosols from the stratospheric reservoir into the upper troposphere occurs quite slowly. Such aerosols can act as cloud condensation nuclei and may influence cloud properties in the upper troposphere over years.

After the eruption of Pinatubo it was for the first time possible to measure optical properties of volcanic aerosol in the stratosphere with the Raman method (2). The Raman method allows for an independent determination of extinction and backscatter coefficients (3). The particle extinction-to-backscatter (lidar) ratio contains information on particle size and particle light-absorption and thus allows for a rough estimation of microphysical parameters of stratospheric aerosols (4).

Table 1. Major volcanic eruptions in the northern hemisphere since July 2008. The information have been obtained from www.avo.alaska.edu and from www.volcanodiscovery.com

volcano	location	plume height
Okmok	Aleutians	15 km
Kasatochi	Aleutians	15.2 km
Shiveluch	Kamchatka	8.8 km
Cleveland	Aleutians	6 km
Redoubt	Alaska	20 km
Sarychev	Kuriles	12 km

The volcanic layers of 2008 and 2009 can be studied in much more detail by the continental-scale network of multi-wavelength Raman lidars of the European Aerosol Research LIdar NETwork EARLINET (6). The wavelength dependence of the backscatter and extinction coefficients and of the lidar ratios allow for a more detailed differentiation of aerosol types and for the direct retrieval of microphysical aerosol parameters like effective radius and single-scattering albedo (7; 8). There was a major effort during the past years to extract characteristic optical properties for different aerosol types from multi-wavelength Raman lidar measurements (8). This kind of aerosol model is used, e.g., for the analysis of data from simple backscatter lidars like the CALIPSO lidar CALIOP. Unfortunately those aerosol models as well as the CALIPSO retrieval algorithm do not yet contain stratospheric aerosols. Studies on the 2008/2009 volcanic layers can fill this gap.

2. INSTRUMENTATION

From measurements with the IfT multi-wavelength Raman lidar we obtain vertical profiles of backscatter coefficients at 355, 532, and 1064 nm, extinction profiles at 355 and 532 nm as well as depolarization ratio profiles at 532 nm. The lidar system and data analysis are

© Proceedings of the 8th International Symposium on Tropospheric Profiling, ISBN 978-90-6960-233-2
Delft, The Netherlands, October 2009. Editors, A. Apituley, H.W.J. Russchenberg, W.A.A. Monna

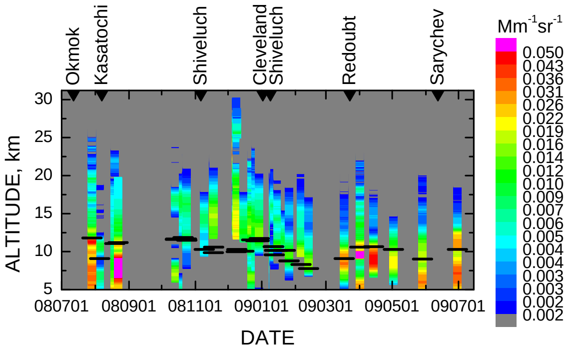

Figure 1. Time series of aerosol layers in the ULTS region in terms of backscatter coefficient at 1064 nm. The individual profiles have been obtained with the Klett method (5). Black lines indicate the tropopause heights of the individual observations. The date is give in the format YYMMDD.

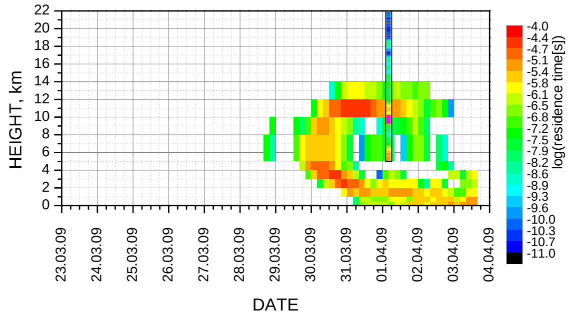

Figure 2. Example for source identification of the aerosol layers. The background shows the result of FLEXPART forward simulation. The color coding indicates the probability that air parcels from the Redoubt eruption on March 23, 2009 arrived over Leipzig. The column within the black frame shows the lidar observation of April 1, 2009 (see Fig 1).

described by (9; 10) and (11).

For aerosol observations in the free-troposphere the relative errors of the particle backscatter and extinction coefficients and the lidar ratio are of the order of 5%–20%, 15%–40%, and 20%–60%, respectively. In some cases the Raman signals in the stratosphere are too noisy and do not allow for an calculation of backscatter and extinction coefficients with the Raman method.

For the documentation of the temporal development of the stratospheric plume we applied the Fernald method (5) to the 1064-nm signals. The signals have been smoothed with window lengths between 1260 and 2400 m. The calibration was performed in such a way that the mean backscatter values are zero above the stratospheric layer. The uncertainty of the derived profiles due to a wrong assumption of the lidar ratio is negligible because of the very low optical depth of the stratospheric layers.

The origin of the aerosol layers in the UTLS region was determined with FLEXPART simulations. FLEXPART is a Lagrangian particle dispersion model (12). It treats long-range transport, dry and wet deposition, turbulent diffusion, and convection. The transport simulations are driven by meteorological analysis data from the Global Forecast Model (GFS) which have a horizontal resolution of 1°x1°. We used archived GFS data with a temporal resolution of 6 hours (13). We performed simulations backward in time (starting at location and time of the lidar observation) as well as simulations forward in time (starting at time and location of the volcanic eruptions). Fig. 2 illustrates an example for a forward simulation of the Redoubt eruption on March 23, 2009.

3. OBSERVATIONS

IfT is an EARLINET station since 2000. That means that we have a scheduled measurement plan with three observation times per week, Mondays around noon and after sunset, and Thursdays after sunset. There are about 10 additionally scheduled measurements per month in the framework of the EARLINET correlative measurements for CALIPSO (6). About half of the scheduled measurements could not be performed because of rain, snow, or fog.

3.1. Time series

Fig. 1 and Fig. 3 show the temporal development of the aerosol load in the UTLS region from July 2008 to July 2009 in terms of backscatter coefficients at 1064 nm. A first aerosol layer in the tropopause region could be observed on July 28, 2008. Transport simulations indicate that these layers probably originated from the Okmok eruption. A very strong aerosol layer in the upper troposphere was detected on August 21, 2008. This layer came probably from the Kasatochi eruption.

The largest vertical extend of about 30 km could be observed on December 8, 2008. In November and December 2008 the upper troposphere was almost clean, but the aerosol content above the tropopause remained almost constant.

Another strong increase of the aerosol load in the tropopause region occurred in spring. Fig. 2 illustrates how the measurement of April 1, 2009 can be attributed to the Redoubt eruption of March 23.

After the eruption of the Sarychev volcano in mid June 2009 we observed several very thin, separated aerosol layers in the stratosphere. Fig. 4 illustrates this behavior. It shows the measurement of July 15, 2009 in comparison to the observation of April 13, 2009. In April we detected a broad layer around 9 km height, but in July there were very thin layers in 12, 15, and 17.5 km. Similar thin layers have been observed also by other EARLINET stations and with CALIPSO. The thin layers dispersed and layer depth increased up to 4 km by the end of July 2009 (see http://polly.tropos.de/martha).

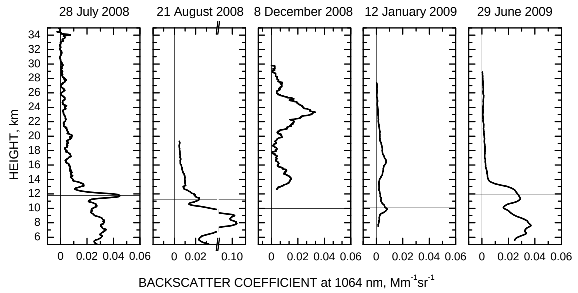

Figure 3. Selected profiles from the time series in Fig 1. The profiles have been obtained with a vertical resolution of approximately 1200 m. Horizontal lines indicate the tropopause heights of the individual observations. The format of the date axis is DD.MM.YY.

After the eruptions of ElChichon and Pinatubo the volcanic plumes arrived over central Europe within the stratosphere. In contrast, during the 2008/2009 event the arriving volcanic plumes seems to 'ignore' the tropopause. They appear below, above, or around the tropopause height. This behaviour may be due to the fact that the 2008/2009 eruptions occured in midlatitudes but not in the tropics.

3.2. Multi-wavelength Raman lidar measurements

Fig. 5 and Table 2 provides example data sets of multi-wavelength Raman lidar data of volcanic aerosols in the UTLS region. In both cases the linear volume depolarization ratios indicate that the layers consisted of spherical particles. The volcanic layer on August 21, 2008 had an optical depth at 532 nm and 355 nm of 0.016 and 0.046, respectively. On January 12, 2009 the values of the optical depths were smaller by a factor of four. On August 21 the aerosol particles were concentrated in the upper troposphere, between 7.5 and 9.7 km height. In contrast, the volcanic plume extended from 7.5 km up to 27.5 km height on January 12 (see Fig. 3).

In both cases the lidar ratios are very uncertain with values of about 34 sr and 45-65 sr at 532 nm and 355 nm, respectively. The extinction coefficients show a strong wavelength dependence with Ångström exponents with values of larger than 2. In both cases the backscatter-related Ångström exponent for the 355-nm-532-nm wavelength range is larger than for the 532-nm-to-1064-nm range. Effective radii are about 0.1μm.

4. SUMMARY AND OUTLOOK

We performed multi-wavelength Raman lidar observations of aerosol layers in the UTLS region over Leipzig. The measurements and their analysis will be continued. We demonstrate that it is possible to derive backscatter and extinction coefficients at multiple wavelengths as well as microphysical aerosol properties from those

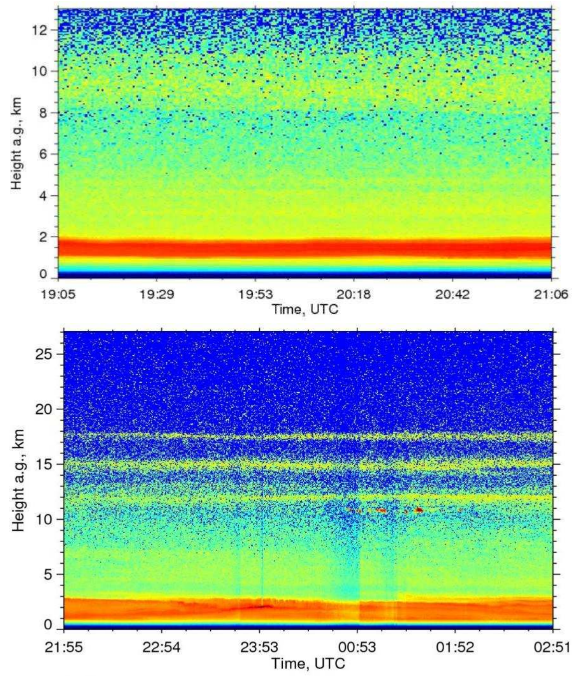

Figure 4. Range-corrected signal at 1064 nm. The observations were performed over Leipzig on April 13, 2009 (top) and July 15, 2009 (bottom).

measurements. This kind of analysis will be applied to more cases of the UTLS measurement series.

The data of all EARLINET stations and of CALIPSO overpasses will be used to study the spatial and temporal variability of the stratospheric layers.

Multi-wavelength observations of the EARLINET Raman lidars can provide input data for an extended aerosol model that contains also stratospheric aerosols. This new model can improve CALIPSO's aerosol type detection algorithm and retrieval algorithm.

ACKNOWLEDGMENTS

The EARLINET-ASOS project is funded by the European Commission (EC) under grant RICA-025991.

The wind fields for the FLEXPART simulations are from the Research Data Archive (RDA) which is maintained by the Computational and Information Systems Laboratory (CISL) at the National Center for Atmospheric Research (NCAR). NCAR is sponsored by the National Science Foundation (NSF). The original data are available from the RDA (http://dss.ucar.edu) in dataset number ds083.2.

REFERENCES

[1] I. Mattis, D. Müller, A. Ansmann, U. Wandinger, J. Preißler, P. Seifert, and M. Tesche, "Ten years of multiwavelength Raman lidar observations of free-tropospheric aerosol layers over central Europe: Geometrical properties and annual cycle,"

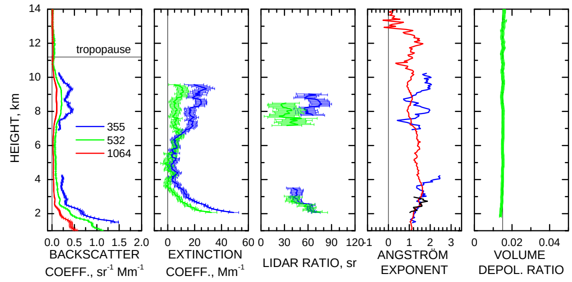

Figure 5. Multi-wavelength Raman lidar observation of volcanic aerosols over Leipzig, Germany, on August 21, 2008, 20:37 - 21:34 UTC.

Table 2. Layer-mean optical properties of the volcanic aerosol layer that has been observed over Leipzig, Germany on January 12, 2009, 16:52 - 18:04 UTC. β denotes the particle backscatter coefficient, α the particle extinction coefficient, S the lidar ratio, $\mathring{a}$ the Ångström exponent, OD the optical depth, and λ the wavelength.

prop.	λ [nm]	value	unit
β	355	15 ± 2	10^{-3} (Mm sr)$^{-1}$
β	532	7 ± 1	10^{-3} (Mm sr)$^{-1}$
β	1064	2.5 ± 0.3	10^{-3} (Mm sr)$^{-1}$
α	355	0.7 ± 0.3	Mm^{-1}
α	532	0.2 ± 0.2	Mm^{-1}
S	355	44 ± 20	sr
S	532	34 ± 23	sr
$\mathring{a}_\beta$	355/532	1.8 ± 0.7	
$\mathring{a}_\beta$	532/1064	1.6 ± 0.4	
$\mathring{a}_\alpha$	355/532	2.5 ± 3	
OD	355	0.01	
OD	532	0.004	

J. Geophys. Res. **113**, doi:10.1029/2007JD009636 (2008).

[2] A. Ansmann, I. Mattis, U. Wandinger, F. Wagner, J. Reichardt, and T. Deshler, "Evolution of the Pinatubo aerosol: Raman lidar observations of particle optical depth, effective radius, mass and surface area over Central Europe at 53.4 °N," J. Atmos. Sci **54**, 2630–2641 (1997).

[3] A. Ansmann, M. Riebesell, U. Wandinger, C. Weitcamp, E. Voss, W. Lahmann, and W. Michaelis, "Combined Raman elastic-backscatter lidar for vertical profiling of moisture, aerosol extinction, backscatter, and lidar ratio," Appl. Phys. B **55**, 18–28 (1992).

[4] U. Wandinger, A. Ansmann, J. Reichardt, and T. Deshler, "Determination of stratospheric aerosol microphysical properties from independent extinction and backscattering measurements with a raman lidar," Appl. Opt. **34**, 8315–8329 (1995).

[5] F. G. Fernald, "Analysis of atmospheric lidar observations: some comments," Appl. Opt. **23**, 652–653 (1984).

[6] G. Pappalardo, U. Wandinger, L. Mona, A. Hiebsch, I. Mattis, A. Amodeo, A. Ansmann, P. Seifert, H. Linné, A. Apituley, L. Alados Arboledas, D. Balis, A. Chaikovsky, G. D'Amico, F. De Tomasi, V. Freudenthaler, E. Giannakaki, A. Giunta, I. Grigorov, M. Iarlori, F. Madonna, R.-E. Mamouri, L. Nasti, A. Papayannis, A. Pietruczuk, M. Pujadas, V. Rizi, F. Rocadenbosch, F. Russo, F. Schnell, N. Spinelli, X. Wang, and M. Wiegner, "EARLINET correlative measurements for CALIPSO: first intercomparison results," J. Geophys. Res. p. submitted (2009).

[7] D. Müller, U. Wandinger, and A. Ansmann, "Microphysical particle parameters from extinction and backscatter lidar data by inversion with regularization: simulation," Appl. Opt. **38**, 2358–2368 (1999).

[8] D. Müller, A. Ansmann, I. Mattis, M. Tesche, U. Wandinger, D. Althausen, and G. Pisani, "Aerosol type dependent lidar-ratio observed with Raman lidar," J. Geophys. Res. **112**, doi:10.1029/2006JD008292 (2007).

[9] I. Mattis, A. Ansmann, D. Althausen, V. Jaenisch, U. Wandinger, D. Müller, Y. F. Arshinov, S. M. Bobrovnikov, and I. B. Serikov, "Relative humidity profiling in the troposphere with a Raman lidar," Appl. Opt. **41**, 6451–6462 (2002).

[10] I. Mattis, A. Ansmann, D. Müller, U. Wandinger, and D. Althausen, "Dual–wavelength Raman lidar observations of the extinction–to–backscatter ratio of Saharan dust," Geophys. Res. Lett. **29**, 10.1029/2002GL014721 (2002).

[11] A. Ansmann, F. Wagner, D. Müller, D. Althausen, A. Herber, W. v. Hoyningen-Huene, and U. Wandinger, "European pollution outbreaks during ACE 2: Optical particle properties inferred from multiwavelength lidar and star-Sun photometry," J. Geophys. Res. **107**, doi:10.1029/2001JD001109 (2002).

[12] A. Stohl and D. Thomson, "A density correction for lagrangian particle dispersion models," Boundary-Layer Meteorol. **90**, 155–167 (1999).

[13] U.S. National Centers for Environmental Prediction, "updated daily: NCEP FNL Operational Model Global Tropospheric Analyses," Dataset ds083.2 published by the CISL Data Support Section at the National Center for Atmospheric Research, Boulder, CO, available online at http://dss.ucar.edu/datasets/ds083.2/ (continuing from July 1999).